The regulatory proteins DSCR6 and Ezh2 oppositely regulate Stat3 transcriptional activity in mesoderm patterning during *Xenopus* development

Received for publication, August 19, 2019, and in revised form, January 15, 2020 Published, Papers in Press, January 29, 2020, DOI 10.1074/jbc.RA119.010719

Mafalda Loreti, De-Li Shi[1], and Clémence Carron[2]

From the Sorbonne Université, CNRS UMR7622, IBPS-Developmental Biology Laboratory, 75005 Paris, France

Edited by Xiao-Fan Wang

Embryonic cell fate specification and axis patterning requires integration of several signaling pathways that orchestrate region-specific gene expression. The transcription factor signal transducer and activator of transcription 3 (Stat3) plays important roles during early development, but it is unclear how Stat3 is activated. Here, using *Xenopus* as a model, we analyzed the post-translational regulation and functional consequences of Stat3 activation in dorsoventral axis patterning. We show that Stat3 phosphorylation, lysine methylation, and transcriptional activity increase before gastrulation and induce ventral mesoderm formation. Down syndrome critical region gene 6 (DSCR6), a RIPPLY family member that induces dorsal mesoderm by releasing repressive polycomb group proteins from chromatin, bound to the Stat3 C-terminal region and antagonized its transcriptional and ventralizing activities by interfering with its lysine methylation. Enhancer of zeste 2 polycomb-repressive complex 2 subunit (Ezh2) also bound to this region; however, its methyltransferase activity was required for Stat3 methylation and activation. Loss of Ezh2 resulted in dorsalization of ventral mesoderm and formation of a secondary axis. Furthermore, interference with Ezh2 phosphorylation also prevented Stat3 lysine methylation and transcriptional activity. Thus, inhibition of either Ezh2 phosphorylation or Stat3 lysine methylation compensated for the absence of DSCR6 function. These results reveal that DSCR6 and Ezh2 critically and post-translationally regulate Stat3 transcriptional activity. Ezh2 promotes Stat3 activation in ventral mesoderm formation independently of epigenetic regulation, whereas DSCR6 specifies dorsal fate by counteracting this ventralizing activity. This antagonism helps pattern the mesoderm along the dorsoventral axis, representing a critical facet of cell identity regulation during development.

Cell fate decision and embryonic axis formation are fundamental events during early development. Mesoderm cells are specified after fertilization as a result of inductive interactions that involve different critical signaling pathways and transcription factors (1). During gastrulation, these cells are further patterned along the dorsoventral (DV)[3] axis in a regionally specific manner to generate different types of mesoderm tissues of the future embryo. It is well-established that this patterning process is governed by antagonistic interactions between signals secreted by the Spemann organizer and the ventral mesoderm (1–4). Transcriptional repression between dorsal and ventral genes also participates in DV patterning and is required for the development of anteroposterior axis (5–7). Furthermore, transcriptional derepression contributes to regulate dorsal mesoderm and embryonic axis formation. In *Xenopus*, DSCR6 physically and functionally interacts with polycomb group (PcG) proteins to prevent their repressive activity on dorsal mesoderm gene expression (8). This suggests that the interaction between PcG proteins and their antagonistic factors plays an important role in DV patterning during early development.

Polycomb repressive complexes (PRC1 and PRC2) are major modulators of histone methylation, promoting either activation or repression of gene expression in a stage- and cell-type specific manner (9–12). They are critically involved in maintaining stem cell pluripotency in developing vertebrate embryos (13–15). Ezh2 is the enzymatic subunit of PRC2, and its histone methyltransferase activity normally catalyzes trimethylation of lysine 27 on Histone H3 (H3K27me3) at target promoters to mediate gene silencing (9, 14). However, there is accumulating evidence demonstrating that Ezh2 also exhibits important nonepigenetic functions. In particular, it directly modulates the activity of a number of transcription factors in cancer progression (16–19). For example, dimethylation of lysine 49 on Stat3 by the same histone-modifying enzyme increases Stat3 transcriptional activity and promotes tumorigenecity (17, 19). This suggests that functional modulation of Ezh2 and Stat3 activity produces critical effects on gene expression and cell identity determination.

Members of the signal transducer and activator of transcription (Stat) family are structurally and functionally related proteins that mediate the functional response and specificity in

This work was supported by the Centre National de la Recherche Scientifique (CNRS), the Sorbonne Université, the Groupement des Entreprises Françaises dans la Lutte contre le Cancer (Gefluc), and a Doctoral Fellowship from the Ministère de l'Enseignement Supérieur et de la Recherche (to M. L.). The authors declare that they have no conflicts of interest with the contents of this article.

This article contains Figs. S1–S5.

[1] To whom correspondence may be addressed. E-mail: de-li.shi@upmc.fr.

[2] To whom correspondence may be addressed. E-mail: clemence.carron_homo@upmc.fr.

[3] The abbreviations used are: DV, dorsoventral; DSCR6, Down syndrome critical region gene 6; PcG, polycomb group; PRC, polycomb repressive complexes; STAT, signal transducer and activator of transcription; Ezh2, enhancer of zeste 2 polycomb-repressive complex 2 subunit; GST, glutathione *S*-transferase; MLC, myosin light chain; CoMO, control morpholino; IP, immunoprecipitation; DAPI, 4′,6-diamidino-2-phenylindole.

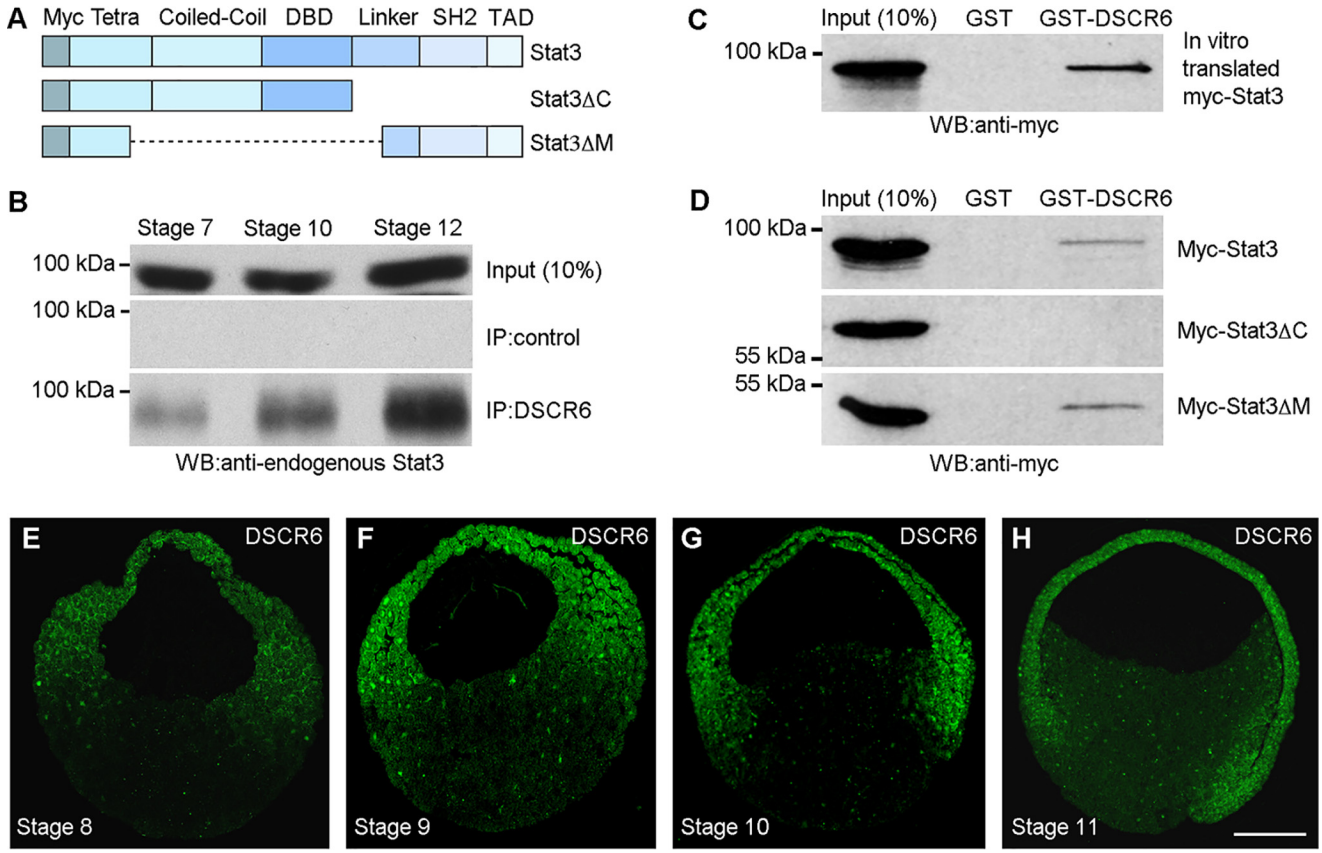

Figure 1. DSCR6 binds to the C-terminal region of Stat3. *A,* schema shows the full-length and truncated Stat3 proteins used for analysis of interaction with DCSR6. *Myc*, 6 myc epitopes at the N terminus; *Tetra*, domain involved in Stat3 tetramerization; *Coiled-coil*, protein interaction domain; *DBD*, DNA-binding domain; *Linker*, linker region; *SH2*, Src homology 2; *TAD*, transactivation domain. *B,* temporal interaction between endogenous DSCR6 and Stat3 in blastula (*stage 7*), early gastrula (*stage 10*), and late gastrula (*stage 12*), analyzed by co-immunoprecipitation using anti-DSCR6 antibody. *C,* GST pulldown of *in vitro* translated Stat3 by GST-DSCR6. *D,* GST pulldown of myc-tagged full-length and truncated Stat3 proteins expressed in the embryos by GST-DSCR6. *E–H,* immunofluorescence staining using anti-DSCR6 antibody shows the expression of endogenous DSCR6 protein in the cytoplasm and nuclei of all three germ layers in blastula (*stages 8* and *9*), early gastrula (*stage 10*), and mid-gastrula (*stage 11*). The sections are oriented with animal pole region up and dorsal region on the *right*. *Scale bar*: *E–H*, 200 μm.

cytokine signaling. They act as pleiotropic transcription factors to regulate cell proliferation and differentiation, immune responses, cell survival, and apoptosis (20–22). Their transcriptional activity is tightly regulated by different post-translational modifications, including acetylation, methylation, phosphorylation, and cellular localization (17, 19, 21, 23). Among different members of this family, Stat3 is constitutively activated in many tumors (24), and is required for cell fate specification (25, 26), embryonic axis formation (27, 28), and cell movements (29–31) during vertebrate early development. However, the mechanism regulating Stat3 activation in these important processes remains largely elusive.

In this study, we analyzed the regulation of Stat3 activation by DSCR6 and Ezh2 in mesoderm patterning using *Xenopus* embryo, which is particularly adapted for functional assays on inductive interactions. We show that both DSCR6 and Ezh2 bind to the C-terminal region of Stat3, forming a regulatory module in DV patterning. Ezh2 methyltransferase function is required for Stat3 transcriptional activity in ventral mesoderm specification. However, DSCR6 antagonizes the ventralizing effect of Stat3 either directly by preventing its activation, or indirectly by interference with Ezh2 function. Furthermore, we find that Ezh2 phosphorylation is required for Stat3 transcriptional activity and ventral mesoderm patterning. This may represent a molecular switch between Ezh2 epigenetic and nonepigenetic functions. Thus, DSCR6 and Ezh2 are important regulators of Stat3 activation in cell fate decisions. Altogether, this work reveals a critical nonepigenetic role of DSCR6 and Ezh2 in the post-translational control of embryonic axis patterning.

Results

Biochemical and functional interactions between DSCR6 and Stat3 in the early embryo

Our previous study has demonstrated that *Xenopus* DSCR6 regulates embryonic axis formation by antagonizing the repressive activity of PcG proteins, including Ezh2 (8). To further understand the regulatory circuit underlying DSCR6-mediated specification of dorsal mesoderm fate, we used a co-immunoprecipitation assay to identify potential DSCR6 partners that repress dorsoanterior development in a similar way as Ezh2. Among different ventralizing factors tested, we found that DSCR6 biochemically interacted with Stat3, whose activation was shown to inhibit dorsal mesoderm formation (27). Stat3 protein comprises different functional domains involved in interaction with other partners and required for its transcriptional activity (Fig. 1*A*). A rabbit antibody against *Xenopus*

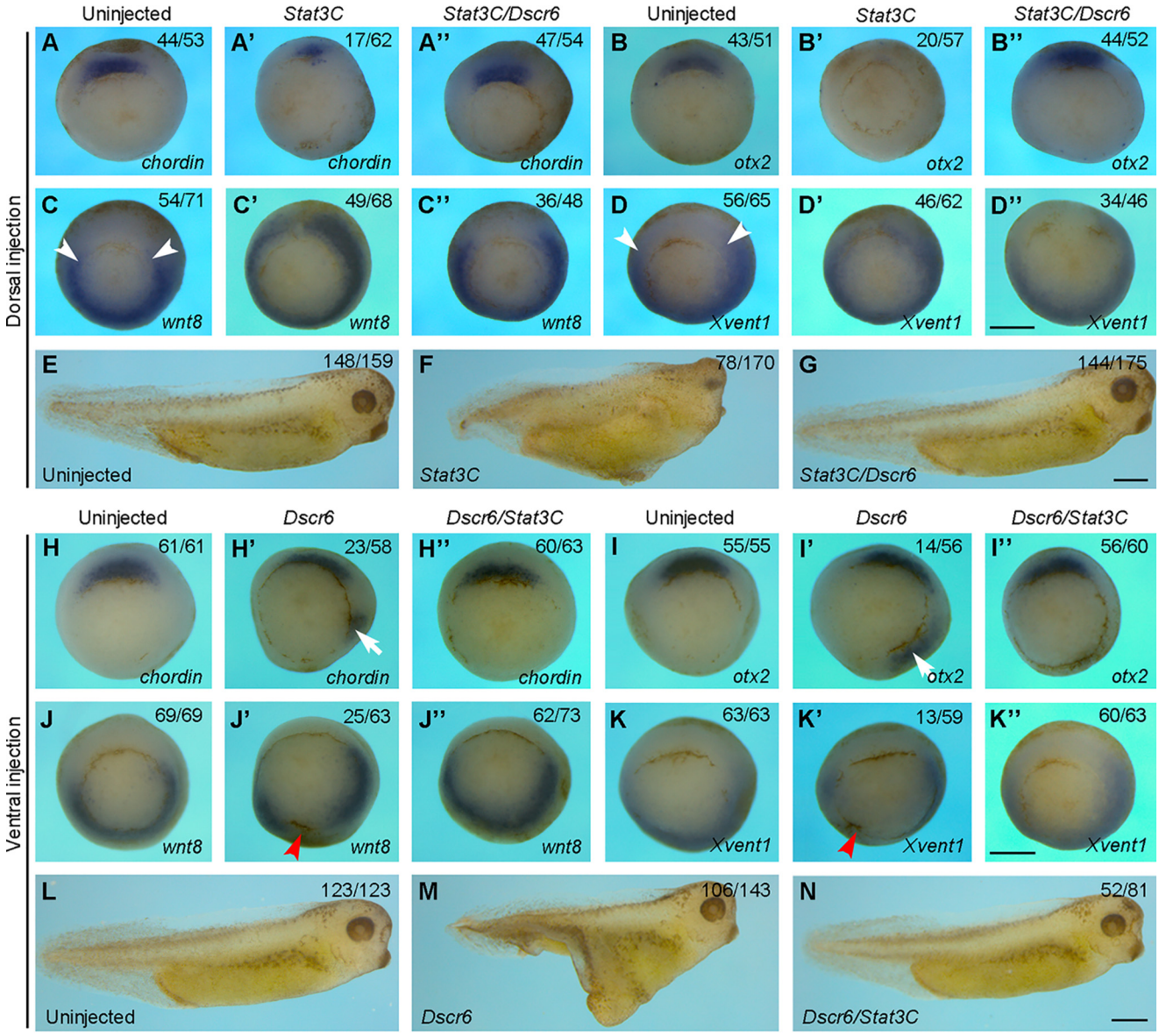

Figure 2. DSCR6 functionally interacts with Stat3 in DV patterning. *A–D″*, *in situ* hybridization analysis shows the expression patterns of dorsal (*chordin* and *otx2*) and ventral (*wnt8* and *Xvent1*) mesoderm genes in early gastrula stage embryos expressing Stat3C or Stat3C and DSCR6 in the dorsal region. *Arrowheads* indicate the dorsal limit of *wnt8* expression in uninjected embryos. All embryos are vegetal view with dorsal region up. *E–G*, live images at larval stage (*stage 36*) show that DSCR6 rescues anterior deficiency produced by dorsal activation of Stat3C. *H–K″*, *in situ* hybridization analysis shows the expression patterns of dorsal and ventral markers in early gastrula stage embryos expressing DSCR6 or DSCR6 and Stat3C in the ventral region. *Arrows* indicate ectopic expression of *chordin* and *otx2*; *arrowheads* show the repression of *wnt8* and *Xvent1* expression. All embryos are vegetal view with dorsal region up. *L–N,* live images at *stage 36* show that DSCR6-induced formation of secondary axis is blocked by activation of Stat3. *Scale bars*: *A–D″*) 500 μm; *E–G,* 500 μm; *H–K″*, 500 μm; *L–N*, 500 μm.

DSCR6 precipitated increasing amounts of endogenous Stat3 protein from blastula to late gastrula stages (Fig. 1*B*). A GST pulldown assay using GST-DSCR6 and *in vitro* translated myc-tagged Stat3 protein further confirmed the physical interaction between DCSR6 and Stat3 (Fig. 1*C*). Next, we set to determine the region in Stat3 required for this interaction, using myc-tagged Stat3 deletion mutants expressed in the embryos following injection of the corresponding mRNAs (500 pg). GST pulldown experiments indicated that GST-DSCR6, but not GST alone, interacted with myc-tagged full-length Stat3, as well as Stat3ΔM lacking the coiled-coil and DNA-binding domains, but it did not interact with Stat3ΔC lacking the linker region, the Src homology 2 domain, and the transactivation domain (Fig. 1*D*). Consistent with the temporal binding between endogenous DSCR6 and Stat3, immunofluorescence staining showed that the DSCR6 protein was localized in the cytoplasm and nuclei of all three germ layers before and during gastrulation (Fig. 1, *E–H*). These results suggest that DSCR6 is expressed at appropriate stages to interact with Stat3 in embryonic patterning.

We then examined how they functionally interact in DV patterning. First, we dorsally expressed Stat3C, a constitutively active form of Stat3 (25), either alone or coexpressed with DSCR6 in the dorsal region of 4-cell stage embryos. When compared with control embryos (Fig. 2, *A* and *B*), dorsal injection of *Stat3C* mRNA (500 pg) inhibited the expression of Spemann organizer genes at early gastrula stage. In severely affected embryos, the expression of *chordin* was strongly reduced

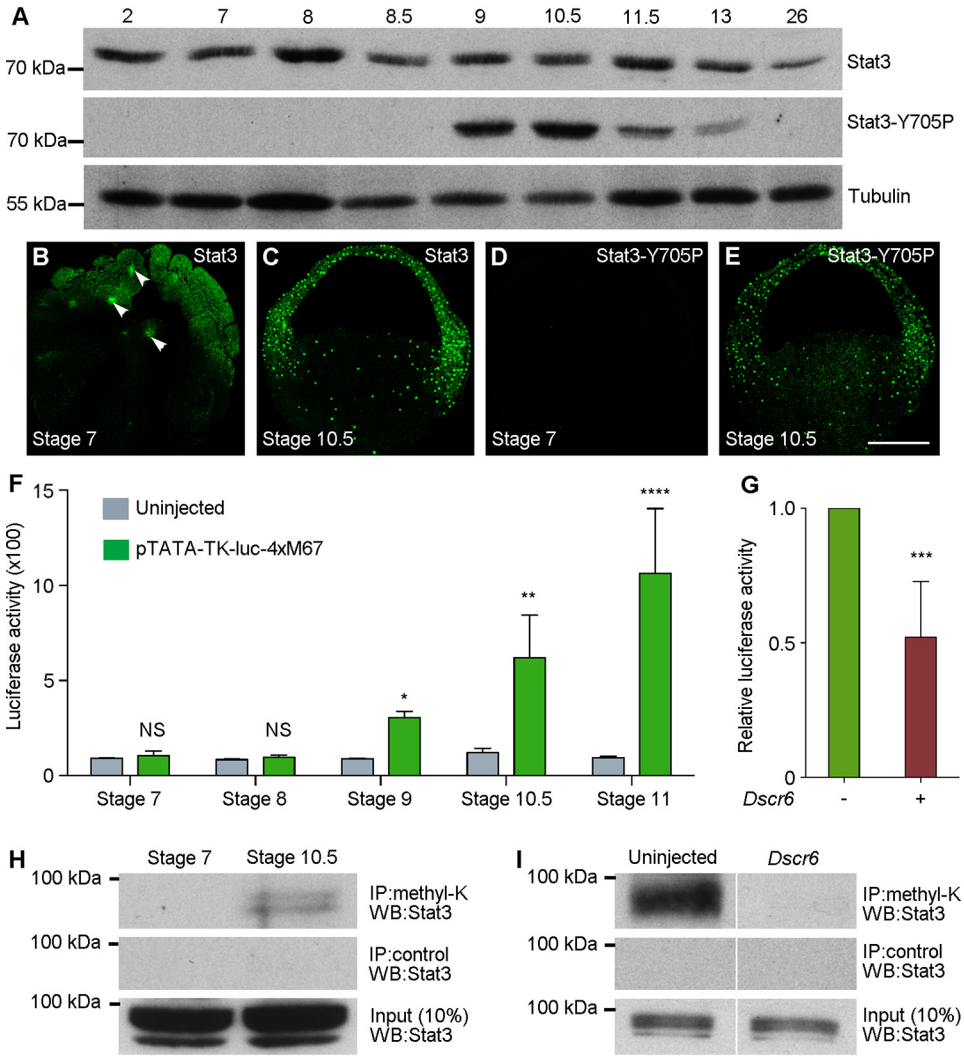

Figure 3. DSCR6 inhibits Stat3 lysine methylation and transcriptional activity. *A,* Western blot analysis shows the temporal expression of endogenous Stat3 and Stat3-Y705P at cleavage (*stage 2*), blastula (*stages 7 to 9*), gastrula (*stages 10.5 to 13*), and tail-bud (*stage 26*) stages. Tubulin is a loading control. *B–E,* apotome microscopic analysis shows the nuclear localization of total Stat3 and Stat3-Y705P in the large-cell blastula (*stage 7*) and early gastrula (*stage 10.5*). *Arrowheads* indicate the nuclear localization of total Stat3 at stage 7. Stat3-Y705P is not present at this stage. *F,* luciferase reporter assay shows temporal Stat3 transcriptional activity (*, $p < 0.05$; **, $p < 0.01$; ****, $p < 0.0001$). *G,* luciferase reporter assay shows the repression of Stat3 transcriptional activity by DSCR6 at early gastrula stage (***, $p < 0.001$). *H,* immunoprecipitation (*IP*) followed by Western blot analysis of lysine-methylated Stat3 protein in the large-cell blastula (*stage 7*) and early gastrula (*stage 10.5*). *I,* DSCR6 represses Stat3 methylation at early gastrula stage. *Scale bar*: *B–E′*, 200 μm.

(Fig. 2*A′*), and the expression of *otx2* was completely blocked (Fig. 2*B′*). Coinjection of *Dscr6* mRNA (100 pg) with *Stat3C* was able to rescue the normal expression pattern of *chordin* and *otx2* in a large majority of embryos (Fig. 2, *A″* and *B″*), indicating an antagonistic interaction between the two proteins. Moreover, in uninjected early gastrula, the expression of *wnt8* and *Xvent1* was detected in lateral and ventral regions (Fig. 2, *C* and *D*), whereas dorsal overexpression of Stat3C could induce their ectopic expression in the Spemann organizer region (Fig. 2, *C′* and *D′*). This was also prevented by coexpression of DSCR6 (Fig. 2, *C″* and *D″*). Consistently, Stat3C-induced anterior deficiency at the tail-bud stage was rescued by DSCR6 (Fig. 2, *E–G*). Conversely, ventral overexpression of DSCR6-induced ectopic expression of *chordin* (Fig. 2, *H* and *H′*), and *otx2* (Fig. 2, *I* and *I′*), this could be counteracted by coexpression of Stat3C (Fig. 2, *H″* and *I″*). In addition, Stat3C was also able to rescue *wnt8* and *Xvent1* expression inhibited by DSCR6 (Fig. 2, *J–K″*). Accordingly, DSCR6-induced formation of the secondary axis was strongly inhibited by Stat3 activation (Fig. 2, *L–N*). These observations suggest that DSCR6 and Stat3 mutually antagonize in DV patterning and embryonic axis formation.

DSCR6 inhibits Stat3 lysine methylation and transcriptional activity

To examine whether the expression and activation of endogenous Stat3 is also consistent with an interaction with DSCR6, we first determined the temporal expression of total Stat3 and Stat3-Y705P by Western blot analysis (Fig. 3*A*). Total Stat3 was expressed at a relatively constant level from early cleavage stage (stage 2) to mid-gastrula stage (stage 11.5), and then decreased from late gastrula stage (stage 13) onward. However, Stat3-Y705P, which is phosphorylated on tyrosine 705 and possesses transcriptional activity, was strongly expressed in the late blastula (stage 9) and early gastrula stages (stage 10.5). Its expression began to decrease in the mid-gastrula (stage 11.5), and was undetectable at the tail-bud stage (stage 26). These were further

confirmed by immunofluorescence staining. In the large-cell blastula (stage 7), total Stat3 was present in the cytoplasm and nuclei (Fig. 3*B*). During gastrulation, it was mostly localized in the nuclei of all three germ layers (Fig. 3*C*). Consistent with Western blot analysis, Stat3-Y705P was absent in the large-cell blastula (Fig. 3*D*). However, its strong nuclear localization in different germ layers was evident in the early gastrula (Fig. 3*E*). Thus, the temporal and spatial activation of Stat3 is consistent with a role in embryonic patterning.

We next directly monitored Stat3 transcriptional activity during early development using the pTATA-TK-Luc-4xM67 luciferase reporter that contains Stat-binding sites (32). Following injection of the reporter (150 pg) at the 2-cell stage, analysis of the promoter-driven reporter activity indicated that it was significantly up-regulated at the late blastula stage (stage 9), and further increased during gastrulation (Fig. 3*F*). To see if this could be influenced by DSCR6, we coinjected *Dscr6* mRNA (500 pg) with the reporter at the 2-cell stage and cultured the embryos to early gastrula stage (stage 10.5). Analysis of the reporter activity showed that it was significantly reduced in the presence of DSCR6 (Fig. 3*G*), suggesting that DSCR6 functions to prevent Stat3 activation.

To provide insights on how DSCR6 regulates Stat3 function, we first examined whether DCSR6 changes the protein level of Stat3 or Stat3-Y705P. Western blot analysis indicated that their expression was not affected following DCSR6 overexpression (Fig. S1). This suggests that DSCR6 inhibits Stat3 transcriptional activity in a phosphorylation-independent manner. Because it has been shown that Stat3 transcriptional activity also depends on lysine methylation (17, 19), we examined whether DSCR6 could influence the protein level of lysine-methylated Stat3. Protein extracts from the large-cell blastula (stage 7) and early gastrula (stage 10.5) were subjected to immunoprecipitation using an antibody for pan-methylated lysine (methyl-K), followed by Western blot analysis using Stat3 antibody. A band of expected size was detected in the early gastrula, but not in the large-cell blastula (Fig. 3*H*). Thus, we conclude that Stat3 becomes lysine-methylated at least at the beginning of gastrulation, which is consistent with the onset of its increased transcriptional activity. Of interest, overexpression of DSCR6 resulted in the disappearance of lysine-methylated Stat3 protein in the early gastrula (Fig. 3*I*). This result raises the possibility that DSCR6 inhibits Stat3 transcriptional activity in ventral mesoderm specification at least in part by preventing its lysine methylation.

Ezh2 binds to the C-terminal region of Stat3

We previously showed that DSCR6 prevents Ezh2-mediated chromatin silencing in mesoderm induction and DV patterning (8). It was also shown that Ezh2 bound to Stat3 in many tumor cells (17, 19). These observations raise the possibility that DSCR6 may either directly regulate Stat3 activation, or indirectly through Ezh2. To examine whether Ezh2 interacts with Stat3, we first determined the expression pattern of Ezh2 protein by Western blotting. Comparable with the temporal expression of Stat3 protein at early stages, the Ezh2 protein level remained constant during cleavage and blastula stages, but increased from mid-gastrula stage onward (Fig. 4*A*). Immunofluorescence staining showed that, as Stat3 and Stat3-Y705P, nuclear localization of Ezh2 was evident in all germ layers of blastula and gastrula stage embryos (Fig. 4, *B–E*). Analysis by co-immunoprecipitation indicated that Ezh2 interacted with endogenous Stat3 at blastula, early and late gastrula stages (Fig. 4*F*). The amount of Stat3 protein precipitated by Ezh2 in the late gastrula was low, probably due to its reduced expression level at this stage. The physical interaction between Ezh2 and Stat3 was further confirmed by a GST pulldown assay using GST-Ezh2 and myc-tagged Stat3 protein produced by *in vitro* translation (Fig. 4*G*). Moreover, by GST pulldown using myc-tagged full-length and truncated Stat3 proteins expressed in the embryos, we extended previous work and showed that Ezh2 bound to the C-terminal region of Stat3 (Fig. 4*H*). Therefore, DSCR6 and Ezh2 independently interact with the same region in Stat3 to regulate its activity.

Ezh2 methyltransferase function is required for Stat3 transcriptional activity in ventral mesoderm specification

To see how Ezh2 and Stat3 functionally interact in DV patterning, we overexpressed a mutant form of Ezh2, Ezh2-H694L, which is enzymatically inactive and acts in a dominant-interfering manner (33). Similarly as DSCR6, injection of synthetic mRNA (500 pg) encoding Ezh2-H694L into ventral blastomeres of 4-cell stage embryos induced the formation of a secondary axis at tail-bud stage, which contained somites, spinal cord, but not notochord (Fig. S2). *In situ* hybridization analysis performed at early gastrula stage indicated that ventral overexpression of Ezh2-H694L induced ectopic expression of *chordin* (Fig. 5, *A* and *A′*) and *otx2* (Fig. 5, *B* and *B′*), and inhibited the expression of *wnt8* (Fig. 5, *C* and *C′*) and *Xvent1* (Fig. 5, *D* and *D′*). These effects were rescued by coexpression of Stat3C (Fig. 5, *A″*, *B″*, *C″*, and *D″*). Consistently, the formation of the secondary axis induced by ventral overexpression of Ezh2-H694L was also inhibited by activation of Stat3 (Fig. 5, *E–G*). These observations clearly show a functional interaction between Ezh2 and Stat3 in DV patterning.

It has been shown that Ezh2 methyltransferase function triggers Stat3 methylation and transcriptional activity in tumor cells (17, 19). To examine whether this regulation operates in the embryo, we first analyzed the effect of blocking Ezh2 enzymatic activity on Stat3 lysine methylation. Embryos at the 2-cell stage were injected with *Ezh2-H694L* mRNA (500 pg), and immunoprecipitation using a pan-methylated lysine antibody followed by Western blot analysis using Stat3 antibody was performed at early gastrula stage. We found that the level of endogenous lysine-methylated Stat3 protein was strongly decreased following inhibition of Ezh2 enzymatic activity, whereas the level of total Stat3 protein was unchanged (Fig. 5, *H* and *I*). Furthermore, we found that the reduced lysine methylation of Stat3 following inhibition of Ezh2 methyltransferase function was correlated with an inhibition of its transcriptional activity. Although WT Ezh2 had no obvious effect on the pTATA-TK-Luc-4xM67 reporter, Ezh2-H694L significantly reduced luciferase activity (Fig. 5*J*), without affecting the expression level and nuclear localization of Stat3-Y705P (Fig. S3). These results suggest that Ezh2 methyltransferase function modulates Stat3 transcriptional activity by changing the state of its lysine meth-

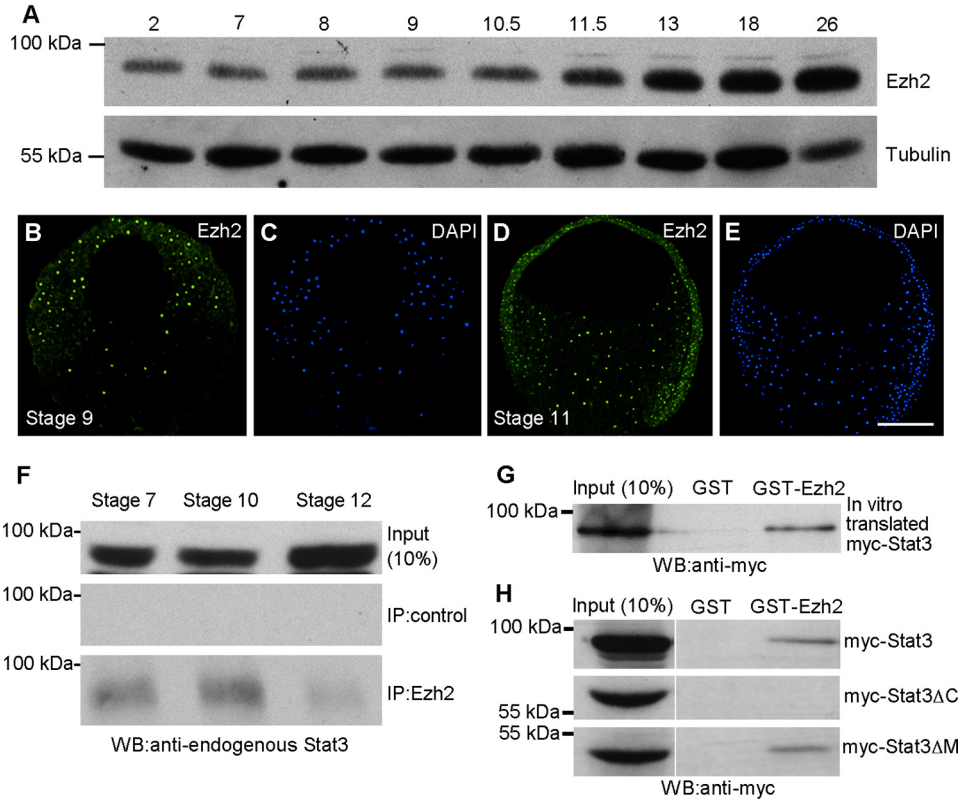

Figure 4. Ezh2 binds to the C-terminal region of Stat3. *A,* Western blot analysis shows the temporal expression of Ezh2 from cleavage to tail-bud stages. Tubulin is a loading control. *B–E,* apotome microscopic analysis shows the nuclear localization of Ezh2 in late blastula (*stage 9*) and mid-gastrula (*stage 11*). *F,* temporal interaction between endogenous Ezh2 and Stat3 in blastula (*stage 7*), early gastrula (*stage 10*), and late gastrula (*stage 12*), analyzed by co-immunoprecipitation using anti-Ezh2 antibody. *G,* GST pulldown of *in vitro* translated myc-tagged Stat3 by GST-Ezh2. *H,* GST pulldown of full-length and truncated Stat3 proteins expressed in the embryos by GST-Ezh2. *Scale bar*: *B–E*, 200 μm.

ylation. Thus, it regulates Stat3 activation in DV patterning through a nonepigenetic mechanism, independently of chromatin silencing.

Ezh2 phosphorylation is required for DV patterning

The fact that overexpression of WT Ezh2 does not change Stat3 transcriptional activity may be due to the lack of its phosphorylation, because it has been shown that Ezh2 phosphorylated on serine 21 (Ezh2-S21P) is required for Stat3 activation (17). To determine whether this indeed regulates Stat3 activation and DV patterning, we first analyzed the localization of Ezh2-S21P at relevant development stages. Immunofluorescence staining using Ezh2-S21P antibody clearly showed that Ezh2-S21P was not present in the large-cell blastula (Fig. 6*A*), but it was strongly accumulated in the nuclei of all three germ layers at the beginning of gastrulation (Fig. 6*B*). Thus, the nuclear localization of Ezh2-S21P correlates well with the increase of Stat3 transcriptional activity. Consistently, injection of synthetic mRNA (500 pg) encoding a constitutively active form of Ezh2, Ezh2-S21D, strongly activated the pTATA-TK-Luc-4xM67 reporter. By contrast, injection of the same amount of mRNA encoding Ezh2-S21A, a nonphosphorylable form of Ezh2, inhibited luciferase activity (Fig. 6*C*). These observations suggest that phosphorylated Ezh2 is present at the right time and right place to regulate Stat3 transcriptional activity.

We next analyzed how Ezh2 phosphorylation is implicated in DV patterning. Synthetic mRNA (500 pg) encoding Ezh2-S21D or Ezh2-S21A was injected into the equatorial region of the two dorsal or ventral blastomeres at 4-cell stages. Overexpression of Ezh2-S21D, but not Ezh2-S21A, in the dorsal region moderately produced anterior deficiency, characterized by the presence of smaller eyes, which generally appeared late during development (Fig. S4). By contrast, overexpression of Ezh2-S21A, but not Ezh2-S21D, in the ventral region induced the formation of a secondary axis in a large majority of embryos (Fig. 6, *D–F*). The induced secondary axis also contained muscles, as assayed by *in situ* hybridization using *myosin light chain* (*MLC*) as a marker (Fig. 6*G*). Thus, inhibition of Stat3 transcriptional activity by Ezh2-H694L is correlated with the specification of dorsal mesoderm fate. This was further supported by overexpression of Stat3-K49R, an inhibitory form of Stat3 in which the substitution of lysine for arginine at position 49 prevents Ezh2 methyltransferase from functioning and results in loss of Stat3 transcriptional activity (19, 34). Injection of the corresponding mRNA (500 pg) in the ventral equatorial region at the 4-cell stage caused the formation of a secondary axis that also only contained muscles (Fig. 6, *H* and *I*). Together, these functional analyses suggest that Ezh2 regulates Stat3 activation in ventral mesoderm specification, whereas DSCR6 promotes dorsal mesoderm formation by antagonizing this ventralizing activity.

To provide further evidence on the functional interaction between DSCR6, Ezh2, and Stat3 in embryonic axis formation,

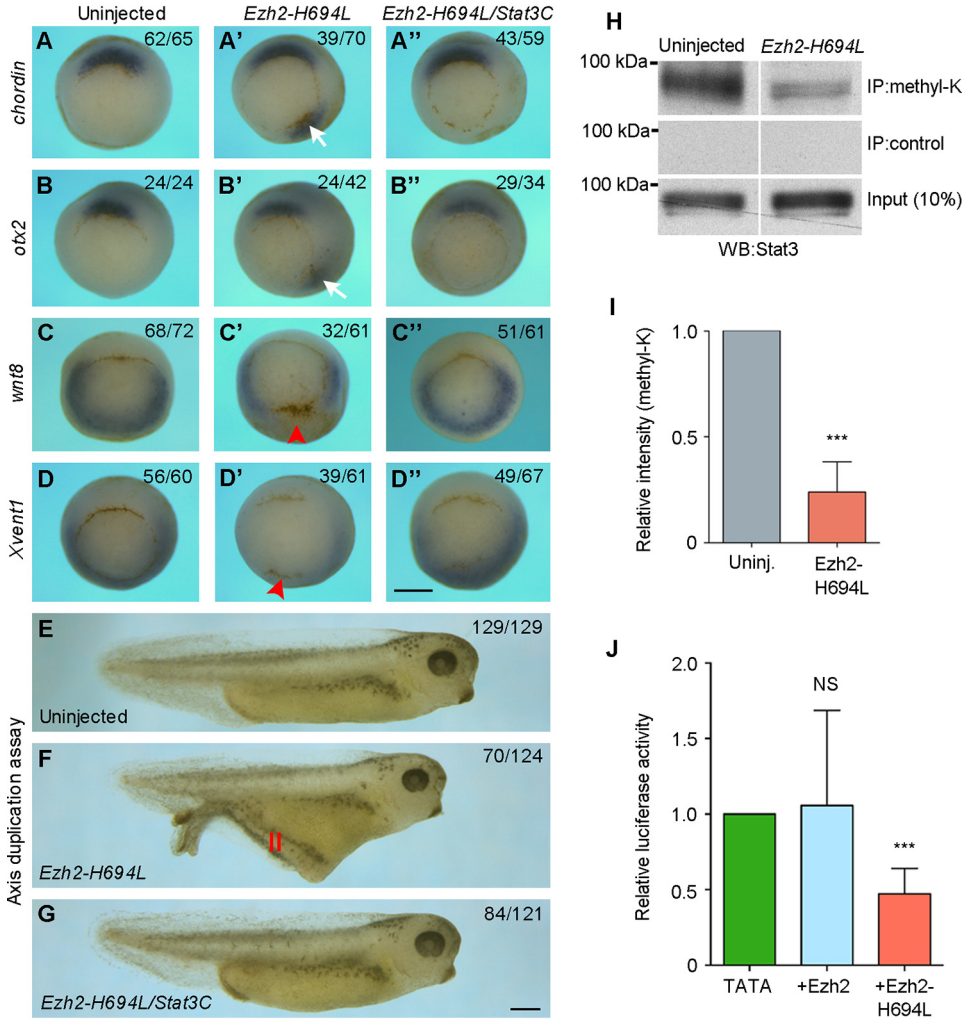

Figure 5. Functional interaction between Ezh2 and Stat3 in DV patterning. *A–D″*, *in situ* hybridization analysis shows the expression of dorsal (*chordin* and *otx2*) and ventral (*wnt8* and *Xvent1*) mesoderm markers in early gastrula expressing Ezh2-H694L or Ezh2-H694L and Stat3C in the ventral region. *Arrows* indicate ectopic expression of *chordin* and *otx2*; *arrowheads* show the region where *wnt8* and *Xvent1* expression is repressed. All embryos are vegetal view with dorsal region up. *E–G,* live images of tail-bud stage embryos. Activation of Stat3 inhibits the formation of secondary axis (*II*) induced by ventral expression of Ezh2-H694L. *H,* Western blot (*WB*) analysis following immunoprecipitation shows the inhibition of Stat3 methylation by Ezh2-H694L at early gastrula stage. *I,* quantification of lysine-methylated Stat3 level (***, $p < 0.001$). *J,* luciferase reporter assay for Stat3 transcriptional activity in early gastrula-stage embryos expressing Ezh2 or Ezh2-H694L (*NS*, not significant; ***, $p < 0.001$). *Scale bars*: *A–D″*, 500 μm; *E–G,* 500 μm.

we examined whether inhibiting the activity of Ezh2 or Stat3 could rescue the phenotype of *Dscr6* morphants. Consistent with our previous observation (8), embryos injected with 40 ng of *Dscr6* morpholino (*Dscr6*MO) developed anterior deficiency, when compared with control morpholino (CoMO)-injected embryos (Fig. 7, *A* and *B*). Overexpression of either Ezh2-H694L or Stat3-K49R by coinjecting the corresponding mRNA (500 pg) efficiently rescued anterior development defects in *Dscr6* morphants (Fig. 7, *C* and *D*). Altogether, our results suggest that DSCR6 specifies dorsal mesoderm fate either by directly preventing the transcriptional activity of Stat3 or indirectly by interfering with Ezh2 methyltransferase function (Fig. 7*E*). Thus, it is clear that DSCR6 and Ezh2 exert opposite activities to post-translationally regulate Stat3 function in DV patterning. However, Stat3 signaling was also able to drive Ezh2 transcriptional activation in gastric cancer (35). To see if this occurs during early development, we overexpressed Stat3C in ectoderm explants and analyzed the expression of *Ezh2* and *Dscr6* at early gastrula stage by RT-PCR. The results showed that the expression of *Ezh2* and *Dscr6* remained unchanged (Fig. S5), this suggests that Stat3 does not feedback to regulate *Ezh2* or *Dscr6* in mesoderm patterning.

Discussion

In this study, we have demonstrated the hierarchical and functional nonepigenetic interactions between DSCR6, Ezh2, and Stat3 during early development. Our results identify DSCR6 and Ezh2 as important and opposite post-translational regulators of Stat3 transcriptional activity. They suggest that Ezh2 methyltransferase functions to promote Stat3 activation through lysine methylation, and this specifies ventral mesoderm fate. By contrast, DSCR6 induces dorsal mesoderm by interfering with Stat3 activation and preventing its ventralizing activity. Thus, we uncover a novel antagonistic action that orchestrates mesoderm patterning.

It has been well-established that PcG proteins function as important modulators that mediates histone methylation (9, 11), and maintains stem cell pluripotency in embryonic stem

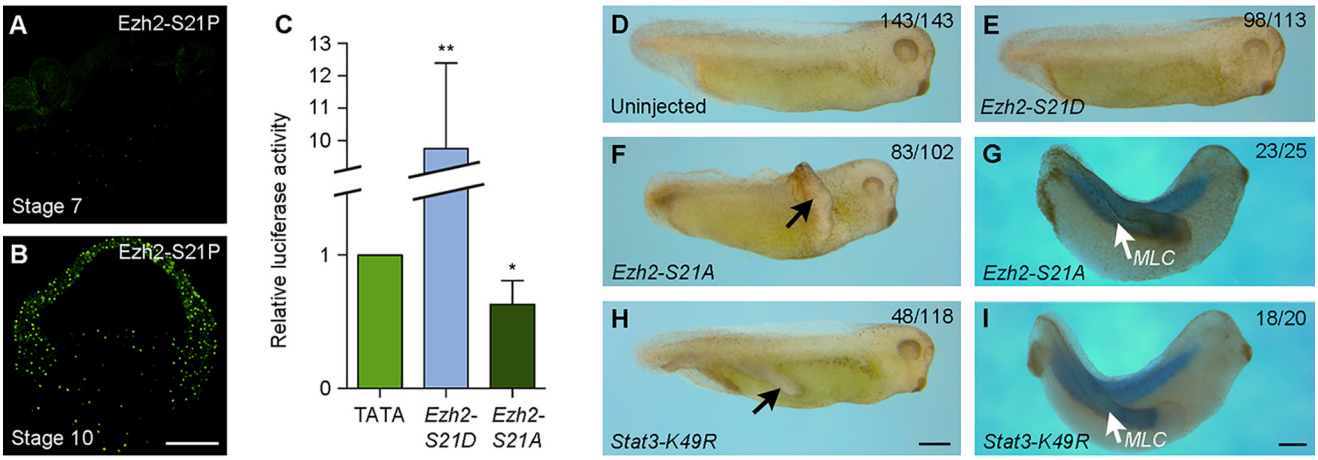

Figure 6. Ezh2 phosphorylation is required for Stat3 methylation and transcriptional activity. *A* and *B*, analysis of the nuclear localization of Ezh2-S21P in the large-cell blastula (*stage 7*) and early gastrula (*stage 10*). *C*, luciferase reporter assay of Stat3 transcriptional activity in early gastrula expressing a constitutively active form of Ezh2, Ezh2-S21D, or a nonphosphorylable form of Ezh2, Ezh2-S21A (*, $p < 0.05$; **, $p < 0.01$). *D*, a control embryo at tail-bud stage. *E*, ventral expression of Ezh2-S21D does not affect embryonic development. *F* and *G*, ventral expression of Ezh2-S21A induces a secondary axis with somitic tissue. *H* and *I*, ventral expression of an inhibitory form of Stat3 methylation, Stat3-K49R, induces a secondary axis with somitic tissue. *Scale bars*: *A* and *B*, 200 μm; *D–F* and *H*, 500 μm; *G* and *I*, 500 μm.

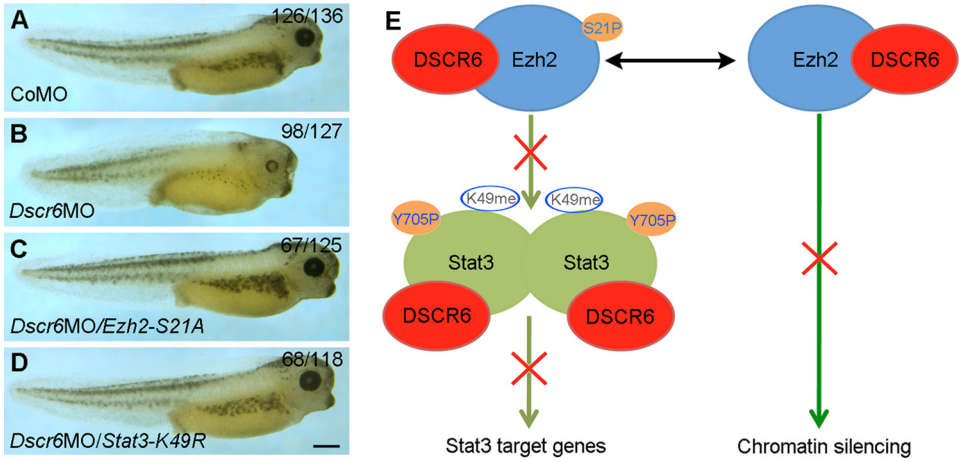

Figure 7. Regulation of Stat3 transcriptional activity by DSCR6 and Ezh2 in embryonic patterning. *A–D*, functional interaction between DSCR6, Ezh2, and Stat3. *A*, a normal larval stage embryo (*stage 40*) previously injected with CoMO. *B*, knockdown of *Dscr6* produces anterior deficiency. *C*, inhibition of Ezh2 phosphorylation by Ezh2-S21A rescues anterior defects in *Dscr6* morphants. *D*, interference with Stat3 lysine methylation by Stat3-K49R rescues anterior defects in *Dscr6* morphants. *E*, a model of functional interaction between DSCR6, Ezh2, and Stat3. Prior to gastrulation, both Ezh2 and Stat3 are phosphorylated and become active. Ezh2 binds to Stat3 and regulates its transcriptional activity through lysine methylation. DSCR6 binds to Ezh2 and Stat3. It may directly interfere with Stat3 transcriptional activity by binding to the C-terminal region that contains protein interaction cassettes and transactivation domain. It may also competitively bind to Ezh2 and interferes with its methyltransferase activity, thus indirectly preventing Stat3 lysine methylation and activation. *Scale bar*: *A–D*, 500 μm.

cells (13–15). Nevertheless, there is accumulating evidence demonstrating that in cancer cells, components of PRC2, particularly Ezh2, can methylate nonhistone proteins, such as GATA4 (36), orphan nuclear receptor RORα (37), androgene receptor (38), and Stat3 (16–19). This methylation plays a critical role in tumorigenesis (39), but its function during development remains unclear. Interestingly, Ezh2-mediated Stat3 lysine methylation also functions in cell fate specification during early development. We show that Ezh2 directly binds to the C-terminal region of Stat3, and its methyltransferase function is implicated in Stat3 lysine methylation that is required for transcriptional activity. This interaction plays a role in specifying the ventral mesoderm fate. Indeed, activation of Ezh2 or Stat3 in the dorsal region inhibits dorsal mesoderm formation and leads to anterior deficiency, whereas interfering with Ezh2 methyltransferase activity or preventing Stat3 from being methylated induces ectopic expression of dorsal mesoderm genes in the ventral mesoderm and leads to the formation of a secondary axis. These effects are consistent with the nuclear localization of active Ezh2 and Stat3 at appropriate stages of early development. Conversely, DSCR6 displays a strong activity to trigger the expression of dorsal genes both in the ventral mesoderm and the naive ectoderm (8). It physically interacts with Ezh2 and Stat3, and inhibits Stat3 transcriptional activity. These strongly suggest that DSCR6 specifies dorsal mesoderm fate by interfering with the ventralizing activity of Ezh2 and Stat3. Thus, dorsal and ventral mesoderm patterning implicates an antagonistic action of DSCR6 on Ezh2 and Stat3, in addition to the already established antagonism mediated by extracellular signals (1).

The present work reveals that Ezh2 regulates Stat3 transcriptional activity in mesoderm patterning independently of epige-

netic repression. Besides its methyltransferase activity, phosphorylated Ezh2 seems to be required for Stat3 activation. Interfering with Ezh2 phosphorylation prevents the ventralizing activity of Ezh2 and induces the formation of a secondary axis, which is mimicked by loss of Stat3 transcriptional activity following substitution of lysine 49 for arginine. Interestingly, it was shown that phosphorylation of Ezh2 on serine 21 inhibits Ezh2 histone methyltransferase activity (40), but enhances Stat3 lysine methylation and transcriptional activity (17). Thus, phosphorylation of serine 21 may represent a molecular switch between Ezh2 epigenetic and nonepigenetic functions.

Besides Ezh2, other components of the PRC2 are also involved in cell lineage commitment during *Xenopus* early development. Mammalian PRC2 consists of three core subunits: SUZ12, EED, and EZH1 or EZH2 (41). Their homologous genes are also expressed during *Xenopus* early development (42, 43). In particular, knockdown of SUZ12 has been shown to affect the expression of early mesoderm genes (44, 45). In *Xenopus*, EED does not seem to regulate mesoderm formation (46), and this is consistent with the observation made in mouse, which shows that EED is required for morphogenetic movements of mesoderm (47). Nevertheless, the reported activity of SUZ12 in regulating the expression of early mesoderm genes is linked to its function in epigenetic repression (45).

Another interesting question concerns the regulation of Stat3 function by DSCR6. At present, there is still no known functional domain identified in RIPPLY family proteins, except a WRPW motif located at the N-terminal region and implicated in interaction with PcG proteins and dorsal mesoderm induction (8). DSCR6 counteracts the ventralizing activity of Stat3, and this is correlated with its ability to inhibit Stat3 lysine methylation and transcriptional activity. There may be at least two possibilities for DSCR6 to interfere with Stat3 function in mesoderm patterning. First, DSCR6 may directly prevent Stat3 activation and repress the expression of its target genes, by binding to the Stat3 C-terminal region that contains protein interaction cassettes and transactivation domain. Second, DSCR6 competitively binds to Ezh2 and interferes with its methyltransferase activity, thus indirectly preventing Stat3 lysine methylation and transcriptional activity. In this regard, our previous work suggests that Ezh2 could recruit DSCR6 through the WRPW tetrapeptide motif, which mediates the interaction between DSCR6 and Ezh2. Furthermore, the WRPW tetrapeptide was able to interfere with Ezh2 activity and induce dorsal mesoderm formation (8). Thus, DSCR6 recruited on PRC2 may either disrupt the complex or interfere with Ezh2 methyltransferase activity. This raises the possibility that DSCR6 may regulate both the epigenetic and nonepigenetic functions of Ezh2 in mesoderm specification. Although the precise mechanism by which DSCR6 regulates Stat3 function in DV patterning remains to be determined, our observations strongly suggest that DSCR6 plays an important role in modulating the nonepigenetic function of Ezh2 on Stat3 transcriptional activity.

The present study reveals that Stat3 lysine methylation mediated by Ezh2 methyltransferase is required for its transcriptional activity in ventral mesoderm fate specification during *Xenopus* development. There is increasing evidence demonstrating that Ezh2 and Stat3 play critical roles in cell lineage commitment and tumorigenesis. In addition to a critical role in maintaining the pluripotency of embryonic stem cells, they are also overexpressed and/or overactivated in different human cancers (16, 48, 49). It is also of note that several genes located within the Down syndrome critical region have been shown to play important roles in regulating various signaling pathways and early developmental processes (8, 50–53). Thus, further analysis of the biochemical and functional interactions between DSCR6, Ezh2, and Stat3 could help to understand the molecular mechanism underlying cell fate decisions and cellular transformation during development and diseases.

Experimental procedures

Embryos

Adult *Xenopus laevis* were maintained in the laboratory, and embryos were obtained and handled as previously described (54). Microinjections were performed using a PLI-100A pneumatic picoliter microinjector (Harvard Apparatus). The experiments were approved by the French Ministère de l'Enseignement Supérieur et de la Recherche (permission number 04845.04).

Plasmid constructs and in vitro mRNA synthesis

The pCS2–6myc-Dscr6, pCS2–6myc-Stat3C, and pCS2–6myc-Ezh2 constructs were previously described (8, 25, 55). The pCS2–6myc-Stat3ΔC and pCS2–6myc-Stat3ΔM constructs were obtained by cloning Stat3 coding region in pCS2-MT vector, followed by deletion of the sequence encoding the last 352 amino acids, or residues 97 to 518, respectively. The pCS2-Stat3-K49R construct was generated by digesting pLEGFP-flag-Stat3-K49R (Addgene) with Xho and SalI, followed by cloning of the insert into the XhoI site of pCS2 vector. The sequence encoding 3myc-Ezh2-H694L was amplified by PCR from the pBabe-puro-3myc-Ezh2-H694L plasmid (33), and cloned into the XhoI site in pCS2 vector. The pcDNA3–3myc-Ezh2-S21A and pcDNA3–3myc-Ezh2-S21D plasmids (40) were digested with BamHI and XhoI to release the inserts, which were then cloned into the corresponding sites in pCS2 vector. All constructs were sequenced before use. Capped mRNAs were synthesized from linearized plasmids by *in vitro* transcription using SP6 RNA polymerase (Thermo Scientific) in the presence of 5′-mGpppG-3′ cap analog (New England Biolabs).

Morpholinos

The *Dscr6* translation-blocking morpholino and the mispair control morpholino (8) were from Gene Tools.

Generation of DSCR6 antibody

The DNQSHMNDKGKPPSF sequence located in the central region of *Xenopus* DSCR6 was used as immunizing peptide. Blast search indicates that it is not conserved among RIPPLY family members, and there is no identical sequence in other proteins. A polyclonal antibody was produced after immunization in rabbit (Eurogentec). The specificity was evaluated by ELISA.

GST pulldown, co-immunoprecipitation, and Western blotting

GST-Ezh2 and GST-Dscr6 constructs were previously described (8), and fusion proteins were produced in *E. coli* cells. Synthetic mRNA (500 pg) encoding myc-tagged full-length or truncated Stat3 proteins was injected into *Xenopus* embryos at the 2-cell stage, and embryonic extracts were prepared at early gastrula stage using GST lysis buffer (100 mM NaCl, 0.5% Nonidet P-40, 5 mM EDTA, 10 mM Tris-HCl, pH 7.5, 2 mM phenylmethylsulfonyl fluoride, 1% aprotinin, 25 μM leupeptin). Alternatively, myc-tagged Stat3 protein was produced by *in vitro* translation using the TNT Coupled Reticulocyte Lysate System (Promega). Lysates were incubated with GSH-agarose (Sigma-Aldrich) overnight at 4 °C, and bound proteins were subjected to Western blot analysis. Control GST pulldown was done using GST beads alone, and 10% of lysates were used as input.

Co-immunoprecipitation experiments were performed using the following antibodies: rabbit anti-DSCR6, rabbit anti-Ezh2 (Abcam), and rabbit anti-pan-methylated lysine (Abcam). Procedures for sample preparation and immunoprecipitation using antibody-conjugated agarose beads were previously described (56). Bound proteins were subjected to Western blot analysis. Control immunoprecipitation was performed using agarose beads alone, and 10% of embryonic extracts were used as input.

For Western blot analysis, embryonic proteins were extracted in ice-cold lysis buffer (57), and separated on SDS-polyacrylamide gel. They were transferred to nitrocellulose membrane and incubated with rabbit anti-Stat3 (Santa Cruz Biotechnology, 1:1,000), mouse anti-Stat3-Y705P (Cell Signaling, 1:2,000), rabbit anti-Ezh2 (Abcam, 1:750), or mouse 9E10 anti-myc (Santa Cruz Biotechnology, 1:1,000), followed by incubation with horseradish peroxidase-conjugated anti-rabbit IgG (Jackson ImmunoResearch Laboratories, 1:10,000) or anti-mouse IgG (Beckman Coulter, 1:10,000). Protein bands were visualized using the Western Lighting Plus-ECL (PerkinElmer Life Sciences), and signals were quantified using ImageJ software.

Immunofluorescence staining

Embryos were collected from early blastula to mid-gastrula stages and fixed in 4% paraformaldehyde overnight at 4 °C. They were embedded in paraffin, and 10-μm sections were cut using a rotary microtome (Leica, MR2125 RTS). Antigen retrieval was conducted by treatment in 10 mM citrate buffer (pH 6.0) at 95–100 °C for 10 min, and sections were permeabilized in methanol at −20 °C for 10 min. After incubation in blocking buffer (0.3% Triton X-100 in 2.5% normal goat serum), sections were incubated overnight at 4 °C with rabbit anti-Stat3-Y705P (Cell Signaling, 1:50), rabbit anti-Stat3 (Santa Cruz Biotechnology, 1:100), rabbit anti-Ezh2 (Abcam, 1:250), or rabbit anti-Ezh2-S21P (Bethyl Laboratories, 1:100). CY3 anti-rabbit IgG (Jackson ImmunoResearch, 1:600) and Alexa Fluor 488-conjugated goat anti-rabbit IgG (INTERCHIM, 1:300) were used as secondary antibodies. Nuclei were stained with 1.5 mg/ml of 4′,6-diamidino-2-phenylindole (DAPI) for 8 min. After several washes in PBS, sections were mounted in Mowiol mounting medium. Images were acquired with a confocal microscope (Leica, SP5), or an apotome microscope (Zeiss).

Luciferase assay

The pTATA-TK-Luc-4xM67 luciferase reporter DNA (150 pg) was mixed with the pRL-TK plasmid DNA (20 pg). They were injected alone or in combination with synthetic mRNA in the animal pole region at the 2-cell stage. Firefly and *Renilla* luciferase activities from five embryos were measured at appropriate stages using the Dual Luciferase Reporter Assay System (Promega). In all experiments, luciferase activity was presented as fold-induction after normalization of firefly to *Renilla* luciferase.

In situ hybridization

Antisense probes were labeled using digoxygenin-labeled rNTP mix (Roche Diagnostics), and BM purple (Roche Diagnostics) was used as a substrate of the alkaline phosphatase (58).

RT-PCR

Total RNAs extracted from whole embryos or ectoderm explants were reverse transcribed using Moloney murine leukemia virus reverse transcriptase (Life Technologies). Semi-quantitative PCR was performed to analyze the expression of *Xenopus Dscr6* and *Ezh2* using specific primers (8, 55).

Statistical analyses

All data were obtained from at least three independent experiments using different batches of embryos. Statistical analysis was performed using unpaired Student's *t* test and GraphPad Prism 6 software, and *p* values are indicated in the corresponding figures and figure legends.

Author contributions—M. L., D.-L. S., and C. C. investigation; D.-L. S. and C. C. conceptualization; D.-L. S. data curation; D.-L. S. and C. C. supervision; D.-L. S. funding acquisition; D.-L. S. and C. C. writing-original draft; D.-L. S. and C. C. project administration.

Acknowledgments—We thank H. Shibuya, M. C. Hung, and M. van Lohuizen for reagents used in this work; the imaging facility at IBPS for help with confocal image acquisition; and E. Mouchel-Viehl, T. Jaffredo, and M. E. Terret for discussion and technical advices.

References

1. Carron, C., and Shi, D. L. (2016) Specification of anteroposterior axis by combinatorial signaling during *Xenopus* development. *Wiley Interdiscip. Rev. Dev. Biol.* **5,** 150–168 CrossRef Medline
2. De Robertis, E. M., Larraín, J., Oelgeschläger, M., and Wessely, O. (2000) The establishment of Spemann's organizer and patterning of the vertebrate embryo. *Nat. Rev. Genet.* **1,** 171–181 CrossRef Medline
3. De Robertis, E. M., and Kuroda, H. (2004) Dorsal-ventral patterning and neural induction in *Xenopus* embryos. *Annu. Rev. Cell Dev. Biol.* **20,** 285–308 CrossRef Medline
4. Niehrs, C. (2004) Regionally specific induction by the Spemann-Mangold organizer. *Nat. Rev. Genet.* **5,** 425–434 CrossRef Medline
5. Gawantka, V., Delius, H., Hirschfeld, K., Blumenstock, C., and Niehrs, C. (1995) Antagonizing the Spemann organizer: role of the homeobox gene *Xvent-1*. *EMBO J.* **14,** 6268–6279 CrossRef Medline
6. Isaacs, H. V., Andreazzoli, M., and Slack, J. M. (1999) Anteroposterior patterning by mutual repression of orthodenticle and caudal-type transcription factors. *Evol. Dev.* **1,** 143–152 CrossRef Medline

7. Cao, J. M., Li, S. Q., Zhang, H. W., and Shi, D. L. (2012) High mobility group B proteins regulate mesoderm formation and dorsoventral patterning during zebrafish and *Xenopus* early development. *Mech. Dev.* **129,** 263–274 CrossRef Medline
8. Li, H. Y., Grifone, R., Saquet, A., Carron, C., and Shi, D. L. (2013) The *Xenopus* homologue of Down syndrome critical region protein 6 drives dorsoanterior gene expression and embryonic axis formation by antagonising polycomb group proteins. *Development* **140,** 4903–4913 CrossRef Medline
9. Cao, R., Wang, L., Wang, H., Xia, L., Erdjument-Bromage, H., Tempst, P., Jones, R. S., and Zhang, Y. (2002) Role of histone H3 lysine 27 methylation in polycomb-group silencing. *Science* **298,** 1039–1043 CrossRef Medline
10. Mohn, F., Weber, M., Rebhan, M., Roloff, T. C., Richter, J., Stadler, M. B., Bibel, M., and Schübeler, D. (2008) Lineage-specific polycomb targets and *de novo* DNA methylation define restriction and potential of neuronal progenitors. *Mol. Cell* **30,** 755–766 CrossRef Medline
11. Margueron, R., and Reinberg, D. (2011) The polycomb complex PRC2 and its mark in life. *Nature* **469,** 343–349 CrossRef Medline
12. Ferrari, K. J., Scelfo, A., Jammula, S., Cuomo, A., Barozzi, I., Stützer, A., Fischle, W., Bonaldi, T., and Pasini, D. (2014) Polycomb-dependent H3K27me1 and H3K27me2 regulate active transcription and enhancer fidelity. *Mol. Cell* **53,** 49–62 CrossRef Medline
13. Boyer, L. A., Plath, K., Zeitlinger, J., Brambrink, T., Medeiros, L. A., Lee, T. I., Levine, S. S., Wernig, M., Tajonar, A., Ray, M. K., Bell, G. W., Otte, A. P., Vidal, M., Gifford, D. K., Young, R. A., and Jaenisch, R. (2006) Polycomb complexes repress developmental regulators in murine embryonic stem cells. *Nature* **441,** 349–353 CrossRef Medline
14. Yu, Y., Deng, P., Yu, B., Szymanski, J. M., Aghaloo, T., Hong, C., and Wang, C. Y. (2017) Inhibition of EZH2 promotes human embryonic stem cell differentiation into mesoderm by reducing H3K27me3. *Stem Cell Reports* **9,** 752–761 CrossRef Medline
15. Shan, Y., Liang, Z., Xing, Q., Zhang, T., Wang, B., Tian, S., Huang, W., Zhang, Y., Yao, J., Zhu, Y., Huang, K., Liu, Y., Wang, X., Chen, Q., Zhang, J., *et al.* (2017) PRC2 specifies ectoderm lineages and maintains pluripotency in primed but not naïve ESCs. *Nat. Commun.* **8,** 672 CrossRef Medline
16. Stark, G. R., Wang, Y., and Lu, T. (2011) Lysine methylation of promoter-bound transcription factors and relevance to cancer. *Cell Res.* **21,** 375–380 CrossRef Medline
17. Kim, E., Kim, M., Woo, D. H., Shin, Y., Shin, J., Chang, N., Oh, Y. T., Kim, H., Rheey, J., Nakano, I., Lee, C., Joo, K. M., Rich, J. N., Nam, D. H., and Lee, J. (2013) Phosphorylation of EZH2 activates STAT3 signaling via STAT3 methylation and promotes tumorigenicity of glioblastoma stem-like cells. *Cancer Cell* **23,** 839–852 CrossRef Medline
18. Dasgupta, M., Unal, H., Willard, B., Yang, J., Karnik, S. S., and Stark, G. R. (2014) Critical role for lysine 685 in gene expression mediated by transcription factor unphosphorylated STAT3. *J. Biol. Chem.* **289,** 30763–30771 CrossRef Medline
19. Dasgupta, M., Dermawan, J. K., Willard, B., and Stark, G. R. (2015) STAT3-driven transcription depends upon the dimethylation of K49 by EZH2. *Proc. Natl. Acad. Sci. U.S.A.* **112,** 3985–3990 CrossRef Medline
20. Ihle, J. N. (2001) The Stat family in cytokine signaling. *Curr. Opin. Cell Biol.* **13,** 211–217 CrossRef Medline
21. Zhuang, S. (2013) Regulation of STAT signaling by acetylation. *Cell Signal.* **25,** 1924–1931 CrossRef Medline
22. Stark, G. R., Cheon, H., and Wang, Y. (2018) Responses to cytokines and interferons that depend upon JAKs and STATs. *Cold Spring Harb. Perspect. Biol.* **10,** a028555 CrossRef Medline
23. Guanizo, A. C., Fernando, C. D., Garama, D. J., and Gough, D. J. (2018) STAT3: a multifaceted oncoprotein. *Growth Factors* **36,** 1–14 CrossRef Medline
24. Frank, D. A. (2007) STAT3 as a central mediator of neoplastic cellular transformation. *Cancer Lett.* **251,** 199–210 CrossRef Medline
25. Ohkawara, B., Shirakabe, K., Hyodo-Miura, J., Matsuo, R., Ueno, N., Matsumoto, K., and Shibuya, H. (2004) Role of the TAK1-NLK-STAT3 pathway in TGF-β-mediated mesoderm induction. *Genes Dev.* **18,** 381–386 CrossRef Medline
26. Nichane, M., Ren, X., and Bellefroid, E. J. (2010) Self-regulation of Stat3 activity coordinates cell-cycle progression and neural crest specification. *EMBO J.* **29,** 55–67 CrossRef Medline
27. Nishinakamura, R., Matsumoto, Y., Matsuda, T., Ariizumi, T., Heike, T., Asashima, M., and Yokota, T. (1999) Activation of Stat3 by cytokine receptor gp130 ventralizes *Xenopus* embryos independent of BMP-4. *Dev. Biol.* **216,** 481–490 CrossRef Medline
28. Jalvy, S., Veschambre, P., Fédou, S., Rezvani, H. R., Thézé, N., and Thiébaud, P. (2019) Leukemia inhibitory factor signaling in *Xenopus* embryo: insights from gain of function analysis and dominant negative mutant of the receptor. *Dev. Biol.* **447,** 200–213 CrossRef Medline
29. Yamashita, S., Miyagi, C., Carmany-Rampey, A., Shimizu, T., Fujii, R., Schier, A. F., and Hirano, T. (2002) Stat3 controls cell movements during zebrafish gastrulation. *Dev. Cell* **2,** 363–375 CrossRef Medline
30. Miyagi, C., Yamashita, S., Ohba, Y., Yoshizaki, H., Matsuda, M., and Hirano, T. (2004) STAT3 noncell-autonomously controls planar cell polarity during zebrafish convergence and extension. *J. Cell Biol.* **166,** 975–981 CrossRef Medline
31. Zhang, T., Yin, C., Qiao, L., Jing, L., Li, H., Xiao, C., Luo, N., Lei, S., Meng, W., Zhu, H., Liu, J., Xu, H., and Mo, X. (2014) Stat3-Efemp2a modulates the fibrillar matrix for cohesive movement of prechordal plate progenitors. *Development* **141,** 4332–4342 CrossRef Medline
32. Besser, D., Bromberg, J. F., Darnell, J. E., Jr., and Hanafusa, H. (1999) A single amino acid substitution in the v-Eyk intracellular domain results in activation of Stat3 and enhances cellular transformation. *Mol. Cell Biol.* **19,** 1401–1409 CrossRef Medline
33. Hernández-Muñoz, I., Taghavi, P., Kuijl, C., Neefjes, J., and van Lohuizen, M. (2005) Association of BMI1 with polycomb bodies is dynamic and requires PRC2/EZH2 and the maintenance DNA methyltransferase DNMT1. *Mol. Cell Biol.* **25,** 11047–11058 CrossRef Medline
34. Yang, J., Huang, J., Dasgupta, M., Sears, N., Miyagi, M., Wang, B., Chance, M. R., Chen, X., Du, Y., Wang, Y., An, L., Wang, Q., Lu, T., Zhang, X., Wang, Z., and Stark, G. R. (2010) Reversible methylation of promoter-bound STAT3 by histone-modifying enzymes. *Proc. Natl. Acad. Sci. U.S.A.* **107,** 21499–21504 CrossRef Medline
35. Pan, Y. M., Wang, C. G., Zhu, M., Xing, R., Cui, J. T., Li, W. M., Yu, D. D., Wang, S. B., Zhu, W., Ye, Y. J., Wu, Y., Wang, S., and Lu, Y. Y. (2016) STAT3 signaling drives EZH2 transcriptional activation and mediates poor prognosis in gastric cancer. *Mol. Cancer* **15,** 79 CrossRef Medline
36. He, A., Shen, X., Ma, Q., Cao, J., von Gise, A., Zhou, P., Wang, G., Marquez, V. E., Orkin, S. H., and Pu, W. T. (2012) PRC2 directly methylates GATA4 and represses its transcriptional activity. *Genes Dev.* **26,** 37–42 CrossRef Medline
37. Lee, J. M., Lee, J. S., Kim, H., Kim, K., Park, H., Kim, J. Y., Lee, S. H., Kim, I. S., Kim, J., Lee, M., Chung, C. H., Seo, S. B., Yoon, J. B., Ko, E., Noh, D. Y., *et al.* (2012) EZH2 generates a methyl degron that is recognized by the DCAF1/DDB1/CUL4E3 ubiquitin ligase complex. *Mol. Cell* **48,** 572–586 CrossRef Medline
38. Xu, K., Wu, Z. J., Groner, A. C., He, H. H., Cai, C., Lis, R. T., Wu, X., Stack, E. C., Loda, M., Liu, T., Xu, H., Cato, L., Thornton, J. E., Gregory, R. I., *et al.* (2012) EZH2 oncogenic activity in castration-resistant prostate cancer cells is Polycomb-independent. *Science* **338,** 1465–1469 CrossRef Medline
39. Hamamoto, R., Saloura, V., and Nakamura, Y. (2015) Critical roles of non-histone protein lysine methylation in human tumorigenesis. *Nat. Rev. Cancer* **15,** 110–124 CrossRef Medline
40. Cha, T. L., Zhou, B. P., Xia, W., Wu, Y., Yang, C. C., Chen, C. T., Ping, B., Otte, A. P., and Hung, M. C. (2005) Akt-mediated phosphorylation of EZH2 suppresses methylation of lysine 27 in histone H3. *Science* **310,** 306–310 CrossRef Medline
41. Deevy, O., and Bracken, A. P. (2019) PRC2 functions in development and congenital disorders. *Development* **146,** dev181354 CrossRef Medline .
42. Aldiri, I., Moore, K. B., Hutcheson, D. A., Zhang, J., and Vetter, M. L. (2013) Polycomb repressive complex PRC2 regulates *Xenopus* retina development downstream of Wnt/β-catenin signaling. *Development* **140,** 2867–2878 CrossRef Medline
43. Tien, C. L., Jones, A., Wang, H., Gerigk, M., Nozell, S., and Chang, C. (2015) Snail2/Slug cooperates with polycomb repressive complex 2

(PRC2) to regulate neural crest development. *Development* **142,** 722–731 CrossRef Medline

44. Peng, J. C., Valouev, A., Swigut, T., Zhang, J., Zhao, Y., Sidow, A., and Wysocka, J. (2009) Jarid2/Jumonji coordinates control of PRC2 enzymatic activity and target gene occupancy in pluripotent cells. *Cell* **139,** 1290–1302 CrossRef Medline
45. Lim, J. W., Hummert, P., Mills, J. C., and Kroll, K. L. (2011) Geminin cooperates with polycomb to restrain multi-lineage commitment in the early embryo. *Development* **138,** 33–44 CrossRef Medline
46. Satijn, D. P., Hamer, K. M., den Blaauwen, J., and Otte, A. P. (2001) The Polycomb group protein EED interacts with YY1, and both proteins induce neural tissue in *Xenopus* embryos. *Mol. Cell Biol.* **21,** 1360–1369 CrossRef Medline
47. Faust, C., Lawson, K. A., Schork, N. J., Thiel, B., and Magnuson, T. (1998) The polycomb-group gene *eed* is required for normal morphogenetic movements during gastrulation in the mouse embryo. *Development* **125,** 4495–4506 Medline
48. Carpenter, R. L., and Lo, H. W. (2014) STAT3 target genes relevant to human cancers. *Cancers* **6,** 897–925 CrossRef Medline
49. Völkel, P., Dupret, B., Le Bourhis, X., and Angrand, P. O. (2015) Diverse involvement of EZH2 in cancer epigenetics. *Am. J. Transl. Res.* **7,** 175–193 Medline
50. Yimlamai, D., Konnikova, L., Moss, L. G., and Jay, D. G. (2005) The zebrafish down syndrome cell adhesion molecule is involved in cell movement during embryogenesis. *Dev. Biol.* **279,** 44–57 CrossRef Medline
51. Shao, M., Liu, Z. Z., Wang, C. D., Li, H. Y., Carron, C., Zhang, H. W., and Shi, D. L. (2009) Down syndrome critical region protein 5 regulates membrane localization of Wnt receptors: Dishevelled stability and convergent extension in vertebrate embryos. *Development* **136,** 2121–2131 CrossRef Medline
52. Hong, J. Y., Park, J. I., Lee, M., Muñoz, W. A., Miller, R. K., Ji, H., Gu, D., Ezan, J., Sokol, S. Y., and McCrea, P. D. (2012) Down's-syndrome-related kinase Dyrk1A modulates the p120-catenin-Kaiso trajectory of the Wnt signaling pathway. *J. Cell Sci.* **125,** 561–569 CrossRef Medline
53. Morales Diaz, H. D. (2014) Down syndrome cell adhesion molecule is important for early development in *Xenopus tropicalis*. *Genesis* **52,** 849–857 CrossRef Medline
54. Li, H. Y., Bourdelas, A., Carron, C., Gomez, C., Boucaut, J. C., and Shi, D. L. (2006) FGF8, Wnt8 and Myf5 are target genes of Tbx6 during anteroposterior specification in *Xenopus* embryo. *Dev. Biol.* **290,** 470–481 CrossRef Medline
55. Barnett, M. W., Seville, R. A., Nijjar, S., Old, R. W., and Jones, E. A. (2001) *Xenopus* Enhancer of Zeste (XEZ); an anteriorly restricted Polycomb gene with a role in neural patterning. *Mech. Dev.* **102,** 157–167 CrossRef Medline
56. Cheng, X. N., Shao, M., Li, J. T., Wang, Y. F., Qi, J., Xu, Z. G., and Shi, D. L. (2017) Leucine repeat adaptor protein 1 interacts with Dishevelled to regulate gastrulation cell movements in zebrafish. *Nat. Commun.* **8,** 1353 CrossRef Medline
57. Cheng, X. N., Shao, M., and Shi, D. L. (2019) Collagen triple helix repeat containing 1a (Cthrc1a) regulates cell adhesion and migration during gastrulation in zebrafish. *Exp. Cell Res.* **381,** 112–120 CrossRef Medline
58. Li, H. Y., Bourdelas, A., Carron, C., and Shi, D. L. (2010) The RNA-binding protein Seb4/RBM24 is a direct target of MyoD and is required for myogenesis during *Xenopus* early development. *Mech. Dev.* **127,** 281–291 CrossRef Medline